

Title	Deposition of moisture barrier films by catalytic CVD using hexamethyldisilazane
Author(s)	Ohdaira, Keisuke; Matsumura, Hideki
Citation	Japanese Journal of Applied Physics, 53(5S1): 05FM03-1-05FM03-4
Issue Date	2014-04-02
Type	Journal Article
Text version	author
URL	http://hdl.handle.net/10119/12138
Rights	This is the author's version of the work. It is posted here by permission of The Japan Society of Applied Physics. Copyright (C) 2014 The Japan Society of Applied Physics. Keisuke Ohdaira and Hideki Matsumura, Japanese Journal of Applied Physics, 53(5S1), 2014, 05FM03-1-05FM03-4. http://dx.doi.org/10.7567/JJAP.53.05FM03
Description	

Deposition of moisture barrier films by catalytic CVD using hexamethyldisilazane

Keisuke Ohdaira and Hideki Matsumura

Japan Advanced Institute of Science and Technology (JAIST),

Nomi, Ishikawa 923-1292, Japan

E-mail: ohdaira@jaist.ac.jp

Hexamethyldisilazane (HMDS) is utilized to deposit moisture barrier films by catalytic chemical vapor deposition (Cat-CVD). An increase in the thickness of silicon oxynitride (SiO_xN_y) films leads to a better water-vapor transmission rate (WVTR), indicating that Cat-CVD SiO_xN_y films deposited using HMDS do not severely suffer from cracking. A WVTR on the order of $10^{-3} \text{ gm}^{-2}\text{day}^{-1}$ can be realized by a Cat-CVD SiO_xN_y film formed using HMDS on a poly(ethylene terephthalate) (PET) substrate without any stacking structures at a substrate temperature of as low as 60 °C. X-ray reflectivity (XRR) measurement reveals that a film density of $>2.0 \text{ g/cm}^3$ is necessary for SiO_xN_y films to demonstrate an effective moisture barrier ability. The use of HMDS will give us safer production of moisture barrier films because of its non-explosive and non-toxic nature.

1. Introduction

High-ability moisture barrier structures are of great importance for the long-term reliability of photovoltaic modules and organic light-emitting diodes (OLEDs).^{1,2)} Although encapsulation using thick glass can realize a sufficient barrier ability, other problems such as heaviness and less flexibility occur. The satisfaction of the required moisture barrier ability by using thin films has thus been desired. Thin films deposited by chemical vapor deposition (CVD) are expected to be a prospective material, since CVD can deposit high-density films at a temperature of less than 100 °C, which is required to avoid thermal damage to organic materials with low thermal tolerance. In particular, catalytic CVD (Cat-CVD), often referred to as hot-wire CVD (HWCVD), can produce thin films suitable for moisture barrier films because of the high gas decomposition rate and the resulting formation of dense films at low temperatures.³⁻⁵⁾ We have so far demonstrated that silicon nitride (SiN_x) and silicon oxynitride (SiO_xN_y) films deposited by Cat-CVD can be utilized as moisture barrier films.⁶⁻⁸⁾ In a conventional system for the deposition of SiN_x films, silane (SiH_4) and ammonia (NH_3) are used as gas sources. The use of SiH_4 , however, is undesirable from the standpoint of safety because of its explosive nature, and the formation of moisture barrier films with a safer material is favorable. We have thus also investigated the formation of moisture barrier films by using hexamethyldisilazane (HMDS), with a molecular formula of $(\text{CH}_3)_3\text{Si-NH-Si}(\text{CH}_3)_3$. HMDS is a non-explosive, non-toxic liquid at room temperature, and can be utilized as a gas source in a Cat-CVD system by vaporizing it to form SiN_x -related films.⁹⁻¹¹⁾ The moisture barrier ability of Cat-CVD SiN_x -related films formed using HMDS is equivalent to that of films formed from SiH_4 .¹⁰⁾ Moreover, unlike in the case of SiH_4 , the addition of O_2 during film

deposition leads to an improvement in the moisture barrier ability.¹⁰⁾ For better understanding of Cat-CVD moisture barrier films formed using HMDS, we have investigated the effect of film thickness and film density on the water-vapor transmission rate (WVTR) in this study. We have found that a film density of $>2.0 \text{ g/cm}^3$ is required for Cat-CVD SiN_x -related films to exhibit an effective barrier ability. An increase in film thickness results in a monotonic reduction in WVTR, meaning that SiN_x -related films formed using HMDS do not severely suffer from cracking.

2. Experimental procedure

We used a cylindrical-shaped Cat-CVD apparatus with a height of $\sim 400 \text{ mm}$ and a diameter of $\sim 500 \text{ mm}$. A tungsten catalyzer heated at $1800 \text{ }^\circ\text{C}$ with a diameter of 0.5 mm and a length of 1250 mm was used for the deposition of SiN_x and SiO_xN_y films. The pressure and substrate temperature during film deposition were fixed at 100 Pa and $60 \text{ }^\circ\text{C}$, respectively. We used HMDS, H_2 , NH_3 , and He-diluted O_2 (2%) as gas sources at various flow rates of 3-24, 0-1000, 0-280, and 0-400 sccm, respectively. A typical deposition rate of SiN_x and SiO_xN_y films was $\sim 10 \text{ nm/min}$. It should be noted that the addition of NH_3 is for tuning nitrogen content in deposited films and for the suppression of the carbonization of the tungsten catalyzer. Figure 1 shows the variation of the resistance of a graphite wire with a diameter of 1.6 mm and a total length of 600 mm heated at $1800 \text{ }^\circ\text{C}$ under H_2 (400 sccm) or NH_3 (280 sccm) flow, which is shown here just for the clear demonstration of the effect of NH_3 addition for the extraction of carbon atoms. When NH_3 gas is introduced to the chamber, the resistance of the graphite wire increases rapidly and continuously. This indicates a shrinkage of the diameter of the graphite wire, indicating the remarkable effect of carbon extraction by NH_3 addition.

Poly(ethylene terephthalate) (PET) was used for substrates to evaluate WVTR. We measured the WVTR of film/PET structures by an equal-pressure method (Illinois Instruments model 7000) under 40 °C and 90% relative humidity (RH). The WVTR of a bare PET substrate was $\sim 4 \text{ gm}^{-2}\text{day}^{-1}$. The thickness of deposited films was evaluated by ellipsometry (at a wavelength of 632.8 nm) for films deposited on crystalline Si wafers. The film density of the deposited films was measured by X-ray reflectivity (XRR). We observed the cross-sectional structure of deposited films by scanning electron microscopy (SEM). The composition of deposited films was evaluated by X-ray photoelectron spectroscopy (XPS).

3. Results and discussion

Figure 2 shows the WVTR of $\text{SiO}_x\text{N}_y/\text{PET}$ structures as a function of film thickness. The SiO_xN_y films were deposited at HMDS, H_2 , NH_3 , and He-diluted O_2 flow rates of 3, 400, 280, and 200 sccm, respectively. The density of the SiO_xN_y films was 2.18 g/cm^3 , which is almost independent of film thickness. One can see a monotonic decrease in WVTR with an increase in film thickness. In general, WVTR is governed both by the diffusion of H_2O molecules in films and by the movement of H_2O through cracks and/or pin-holes, and if the latter is more dominant, the increase in film thickness does not contribute to the improvement in WVTR.¹²⁾ The result shown in Fig. 2 thus indicates that Cat-CVD SiO_xN_y films deposited by using HMDS do not seriously suffer from cracks or pinholes. If film thickness increases to more than 1 μm , we can obtain a WVTR on the order of $10^{-3} \text{ gm}^{-2}\text{day}^{-1}$, without any film stacking. This value meets the WVTR required for application to food packaging, electrophoretic displays, and liquid-crystal displays.^{13,14)} According to Fick's law, the WVTR of a

film without cracks or pinholes can be expressed as

$$j = -D \frac{dn}{dx} = DS \frac{p_{in} - p_{out}}{d}, \quad (1)$$

where j , D , n , S , d , p_{in} , and p_{out} represent the WVTR, diffusion coefficient, H₂O density, solubility coefficient, film thickness, and partial pressures of H₂O at the inlet and outlet sides, respectively.¹⁵⁾ The permeability coefficient (P) of the film material can be defined as

$$P = \frac{jD}{p_{in} - p_{out}}. \quad (2)$$

Since the samples in this study are stacked structures consisting of PET and SiN_x-related films, the total permeability coefficient (P_{total}) of the stacked structures should be shown, which can be written as

$$\frac{P_{total}}{d} = \frac{1}{\frac{d_{PET}}{P_{PET}} + \frac{d_{film}}{P_{film}}} = \frac{j}{p_{in} - p_{out}}, \quad (3)$$

where d_{PET} and d_{film} represent the thickness of a PET substrate and a deposited film, respectively, and P_{PET} and P_{film} are the permeability coefficient of the PET and film material, respectively.¹³⁾ Since d_{PET} , P_{PET} , P_{film} , p_{in} , and p_{out} are fixed values here, the relationship between WVTR (j) and d_{film} can be written as

$$j = \frac{1}{C_1 + C_2 d_{film}}, \quad (4)$$

where C_1 and C_2 are fixed values of $(d_{PET}/P_{PET})/(p_{in} - p_{out})$ and $(1/P_{film})/(p_{in} - p_{out})$, respectively. The solid line in Fig. 2 is the fitting result obtained using Eq. (4). The experimental plots are well fitted by Eq. (4). Since Eq. (4) is true only when cracks or pinholes do not dominate WVTR, we can conclude that Cat-CVD SiO_xN_y films formed using HMDS do not suffer from cracks or pinholes.

Figure 3 shows the cross-sectional SEM image of $\text{SiO}_x\text{N}_y/\text{SiN}_x$ stacked films formed by Cat-CVD using HMDS on an Al film. The SiN_x and SiO_xN_y films were deposited at HMDS, H_2 , NH_3 , and He-diluted O_2 flow rates of 3, 400, 280, and 0 or 200 sccm, respectively. We have previously reported crack generation in a Cat-CVD SiN_x film formed by Cat-CVD using SiH_4 gas, which is the reason for the necessity of stacking structures in our previous study.⁶⁾ In contrast, we can see no cracks in the films formed from HMDS. This result is consistent with the thickness dependence of WVTR shown in Fig. 2. We can thus utilize SiN_x and SiO_xN_y films as moisture barrier films without any stacked structures. The absence of cracks in films deposited using HMDS is probably due to compressive stress. Cat-CVD SiN_x films formed using SiH_4 generally have tensile stress,^{16,17)} and thus are likely to be cracked. In contrast, according to the experimental result of film stress measurement based on Si wafer warpage, SiN_x and SiO_xN_y films formed using HMDS have compressive stress, typically ~ 400 and ~ 100 MPa, respectively, and are thus resistant to cracking, which leads to the formation of crack-free films even for thick films.

Figure 4 shows the WVTR of SiN_x/PET or $\text{SiO}_x\text{N}_y/\text{PET}$ structures as a function of film density. The flow rates of HMDS, H_2 , NH_3 , and He-diluted O_2 were widely changed in the range of 3-24, 0-1000, 0-280, and 0-400 sccm, respectively. The thickness of SiN_x and SiO_xN_y films is approximately 100 nm. Only films with a density of $>\sim 2.0$ g/cm^3 can effectively reduce the WVTR compared with a bare PET substrate, otherwise no moisture barrier ability can be obtained. This finding clearly shows that not only the suppression of crack generation but the densification of the film material itself is important to realize

good moisture barrier films.

Figure 5 shows the WVTR and film density of $\text{SiO}_x\text{N}_y/\text{PET}$ structures as a function of O_2 flow rate. The flow rates of HMDS, H_2 , and NH_3 were 3, 100, and 280 sccm, respectively. The addition of a suitable amount of O_2 can improve the moisture barrier ability when HMDS is utilized as a gas source, unlike the case of films formed using SiH_4 .^{6,10)} According to Fig. 5, the improvement in WVTR is accompanied by the densification of films. The formation of denser films by adding a suitable amount of O_2 may be due to the extraction of carbon atoms from the films. HMDS molecules contain a number of carbon atoms, and are known to be decomposed to $(\text{CH}_3)_3\text{SiNH}$ and $(\text{CH}_3)_3\text{Si}$ radicals on a heated tungsten catalyzer.¹¹⁾ The deposited films thus contain a considerable number of carbon atoms, which is confirmed in the XPS spectra shown in Fig. 6, and the densification of films is inhibited. The number of incorporated carbon atoms, however, decreases by adding O_2 , as shown in Fig. 6. This may be due to the extraction of carbon atoms by forming carbon-oxygen complexes during film deposition. A similar tendency has also been confirmed in the case of plasma-enhanced CVD (PECVD) SiO_xN_y films using HMDS.¹⁸⁾ The decrease in carbon content leads to the formation of denser films and results in a better WVTR. We also hypothesize that the presence of a suitable amount of carbon atoms in the films might be the cause of compressive stress. Figure 6 also shows that the addition of O_2 also leads to a decrease in the number of N atoms in the films. It should be mentioned that the N reduction probably does not contribute to the increase in film density, since the density of stoichiometric a-SiN_x is generally much higher than that of stoichiometric a-SiO_x .

4. Conclusions

Crack-free SiO_xN_y films can be formed by Cat-CVD using HMDS, which leads to a better WVTR particularly for thick films. A WVTR of $4 \times 10^{-3} \text{ gm}^{-2}\text{day}^{-1}$ can be realized by thickening a SiO_xN_y film on a PET substrate without any stacking structures at a substrate temperature of as low as 60°C . A clear relationship between WVTR and film density is confirmed, and a film density of $>2.0 \text{ g/cm}^3$ is necessary for an effective moisture barrier. The addition of a suitable amount of O_2 during film deposition leads to the formation of denser films, resulting in a better WVTR.

Acknowledgments

The authors would like to thank N. Toda and Y. Ohta of JAIST for their support in the experiments. This work was in part supported by the New Energy and Industrial Technology Development Organization (NEDO).

References

- 1) C. R. Osterwald and T. J. McMahon, Prog. Photovoltaics **17**, 11 (2009).
- 2) J. S. Lewis and M. S. Weaver, IEEE J. Sel. Top. Quantum Electron. **10**, 45 (2004).
- 3) H. Matsumura, A. Masuda, and H. Umemoto, Thin Solid Films **501**, 58 (2006).
- 4) H. Nakayama and M. Ito, Thin Solid Films **519**, 4483 (2011).
- 5) D. Spee, K. van der Werf, J. Rath, and R. Schropp, Phys. Status Solidi: Rapid Res. Lett. **6**, 151 (2012).
- 6) Y. Ogawa, K. Ohdaira, T. Oyaidu, and H. Matsumura, Thin Solid Films **516**, 611 (2008).

- 7) K. Saitoh, R. S. Kumar, S. Chua, A. Masuda, and H. Matsumura, *Thin Solid Films* **516**, 607 (2008).
- 8) A. Heya, T. Niki, M. Takano, Y. Yonezawa, T. Minamikawa, S. Muroi, S. Minami, T. Ikari, A. Izumi, A. Masuda, H. Umemoto, and H. Matsumura, *Jpn. J. Appl. Phys.* **44**, 1923 (2005).
- 9) A. Izumi and K. Oda, *Thin Solid Films* **501**, 195 (2006).
- 10) T. Oyaidu, Y. Ogawa, K. Tsurumaki, K. Ohdaira, and H. Matsumura, *Thin Solid Films* **516**, 604 (2008).
- 11) T. Morimoto, S. G. Ansari, K. Yoneyama, T. Nakajima, A. Masuda, H. Matsumura, M. Nakamura, and H. Umemoto, *Jpn. J. Appl. Phys.* **45**, 961 (2006).
- 12) A. P. Roberts, B. M. Henry, A. P. Sutton, C. R. M. Grovenor, G. A. D. Briggs, T. Miyamoto, M. Kano, Y. Tsukahara, and M. Yanaka, *J. Membrane Sci.* **208**, 75 (2002).
- 13) J. Lewis, *Mater. Today* **9**, 38 (2006).
- 14) C. Wang, P.-C. Lai, S. H. Syu, and J. Leu, *Surf. Coatings Technol.* **206**, 318 (2011).
- 15) A. Gruniger and Ph. R. von Rohr, *Thin Solid Films* **459**, 308 (2004).
- 16) M. Takano, T. Niki, A. Heya, T. Osono, Y. Yonezawa, T. Minamikawa, S. Muroi, S. Minami, A. Masuda, H. Umemoto, and H. Matsumura, *Jpn. J. Appl. Phys.* **44**, 4098 (2005).
- 17) T. Tsutsumi, H. Yanagihara, H. Amanai, S. Yoshida, Y. Watanabe, K. Ohdaira, and H. Matsumura, *Annu. Tech. Conf. Proc. - Soc. Vac. Coaters* **55**, 481 (2012).
- 18) J. H. Lee, C. H. Jeong, H. B. Kim, J. T. Lim, S. J. Kyung, and G. Y. Yeom, *Thin Solid Films* **515**, 917 (2006).

Figure captions

Fig. 1. Resistance variation of a graphite wire at a constant current under NH_3 or H_2 flow. Pressure, NH_3 flow rate, H_2 flow rate, and wire temperature were set to be 100 Pa, 280 sccm, 400 sccm, and 1800 °C, respectively.

Fig. 2. WVTR of $\text{SiO}_x\text{N}_y/\text{PET}$ structures as a function of SiO_xN_y film thickness. The circles and solid line represent the experimental data and fitting result obtained using Eq. (4), respectively. The SiO_xN_y films were deposited at a pressure of 100 Pa and at HMDS, H_2 , NH_3 , and He-diluted O_2 flow rates of 3, 400, 280, and 200 sccm, respectively.

Fig. 3. Cross-sectional SEM image of $\text{SiO}_x\text{N}_y/\text{SiN}_x$ stacked films formed on Al films by Cat-CVD using HMDS gas.

Fig. 4. WVTR of SiN_x/PET or $\text{SiO}_x\text{N}_y/\text{PET}$ structures as a function of film density. The film thickness is approximately 100 nm. The flow rates of HMDS, H_2 , NH_3 , and He-diluted O_2 were widely changed in the ranges of 3-24, 0-1000, 0-280, and 0-400 sccm, respectively.

Fig. 5. WVTR and film density of $\text{SiO}_x\text{N}_y/\text{PET}$ structures as a function of He-diluted O_2 flow rate. The flow rates of HMDS, H_2 , and NH_3 were 3, 100, and 280 sccm, respectively.

Fig. 6. (Color online) XPS spectra of Cat-CVD SiN_x and SiO_xN_y films formed using HMDS at various He-diluted O_2 flow rates.

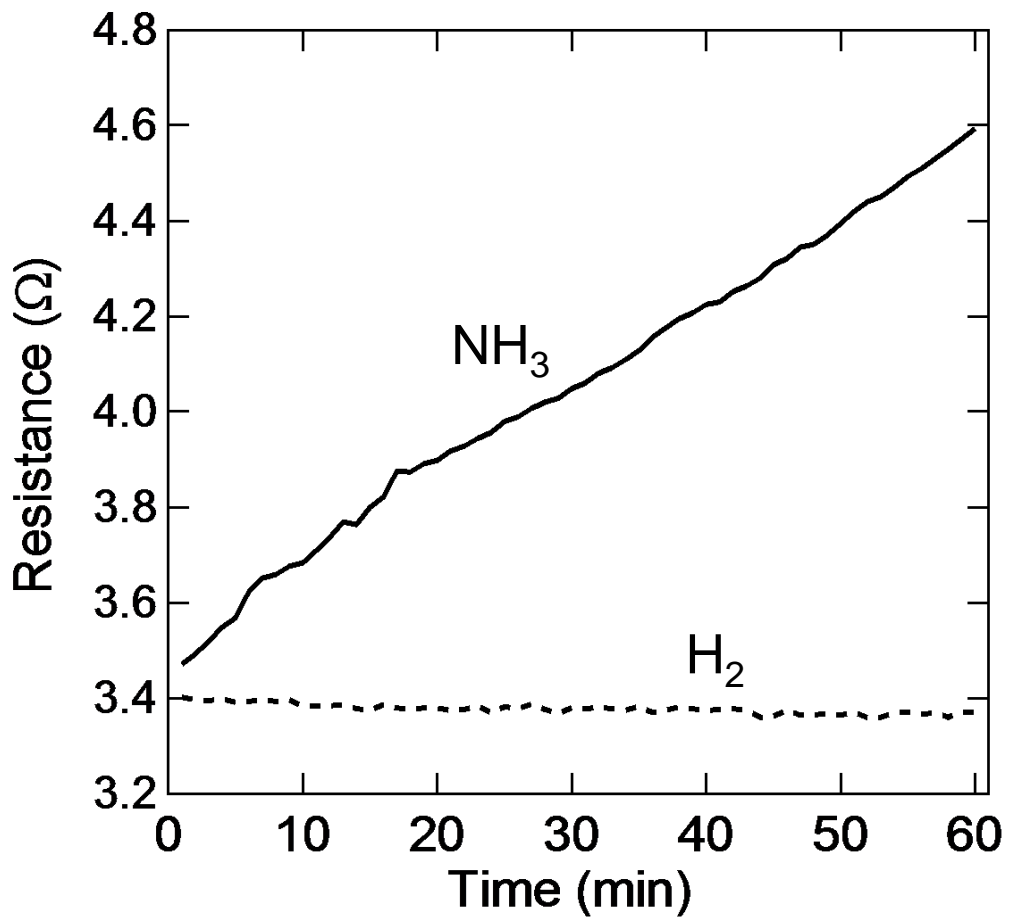


Figure 1 K. Ohdaira *et al.*,

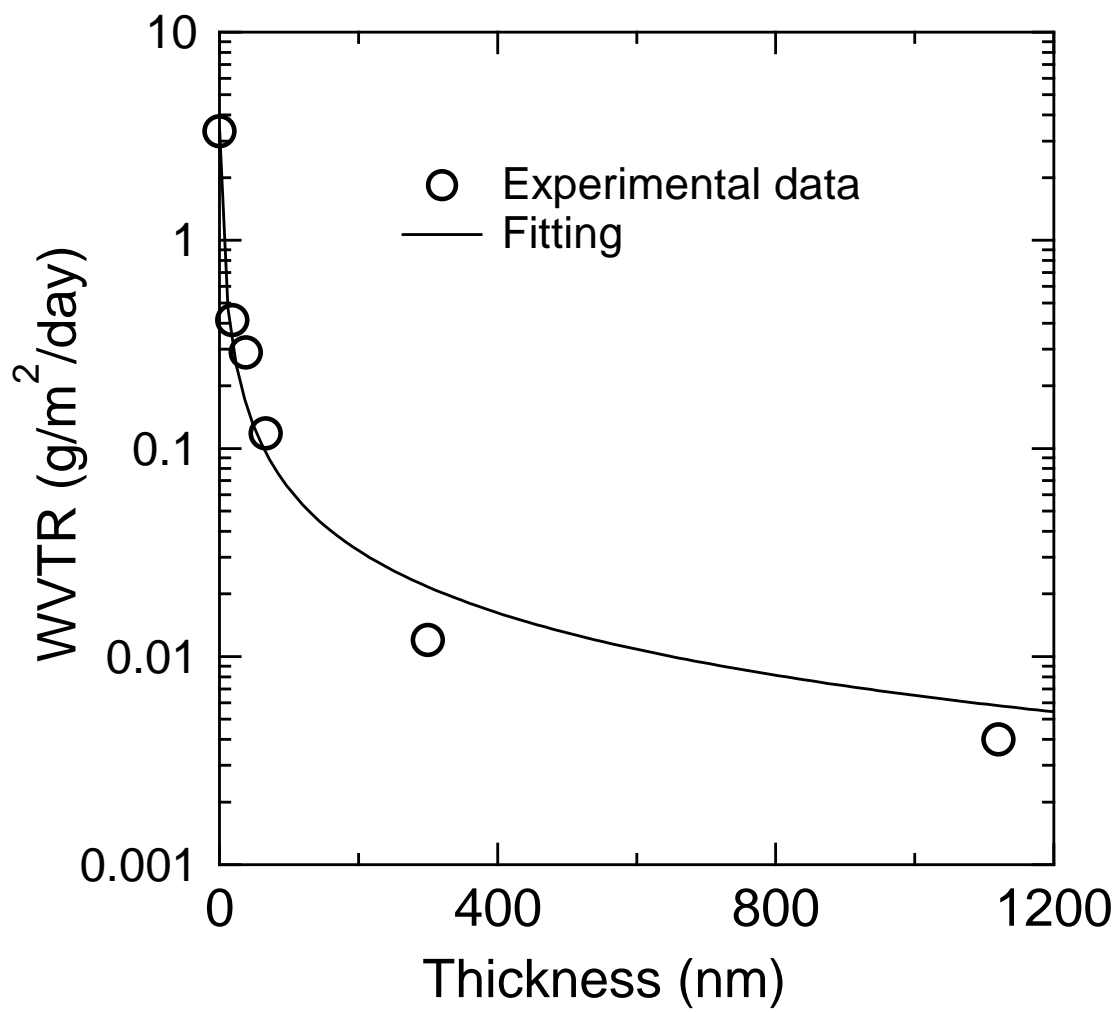


Figure 2 K. Ohdaira *et al.*,

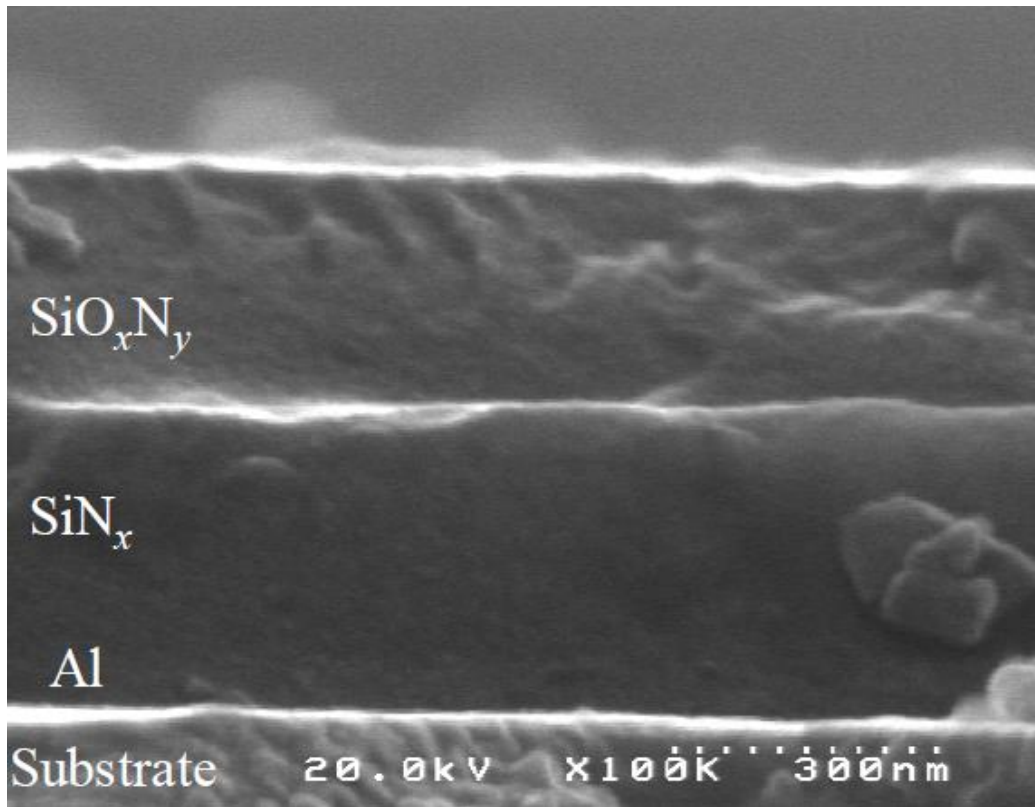


Figure 3 K. Ohdaira *et al.*,

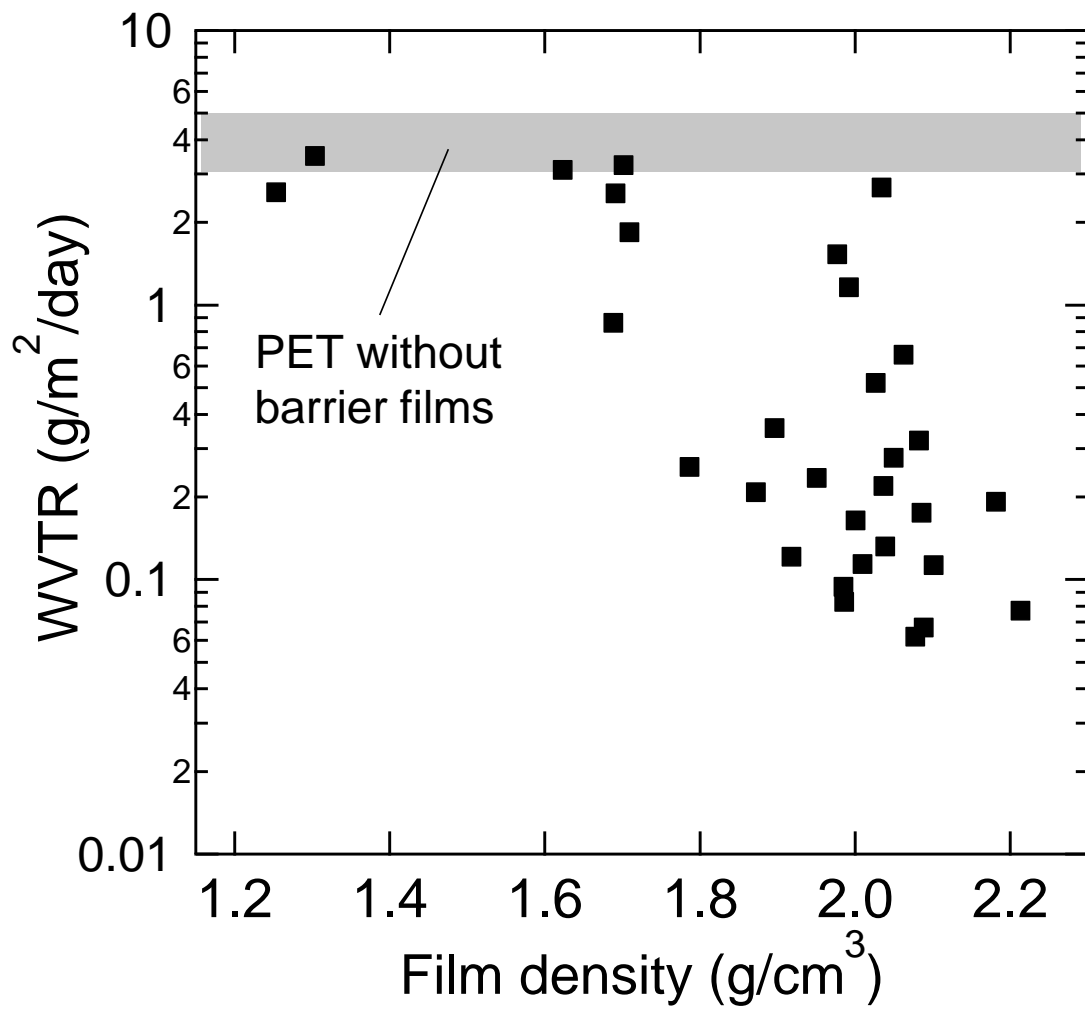


Figure 4 K. Ohdaira *et al.*,

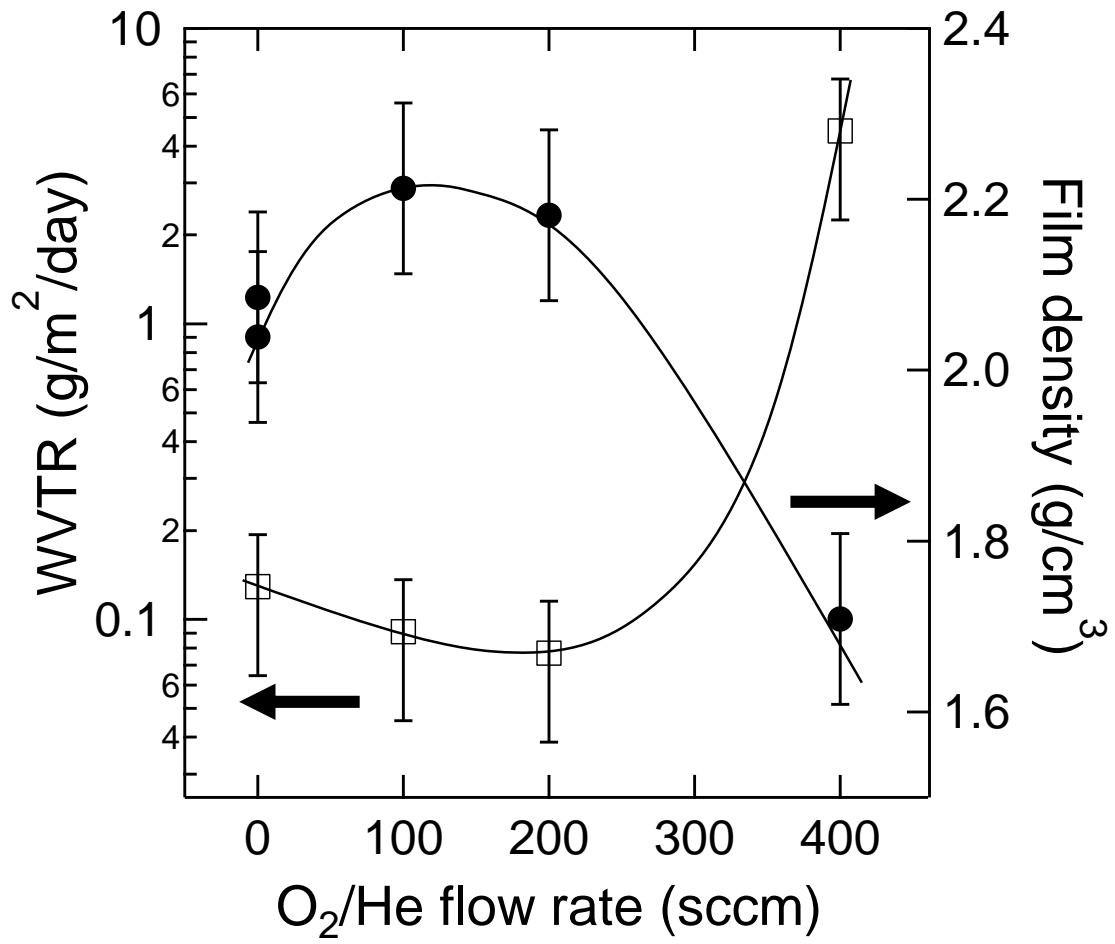


Figure 5 K. Ohdaira *et al.*,

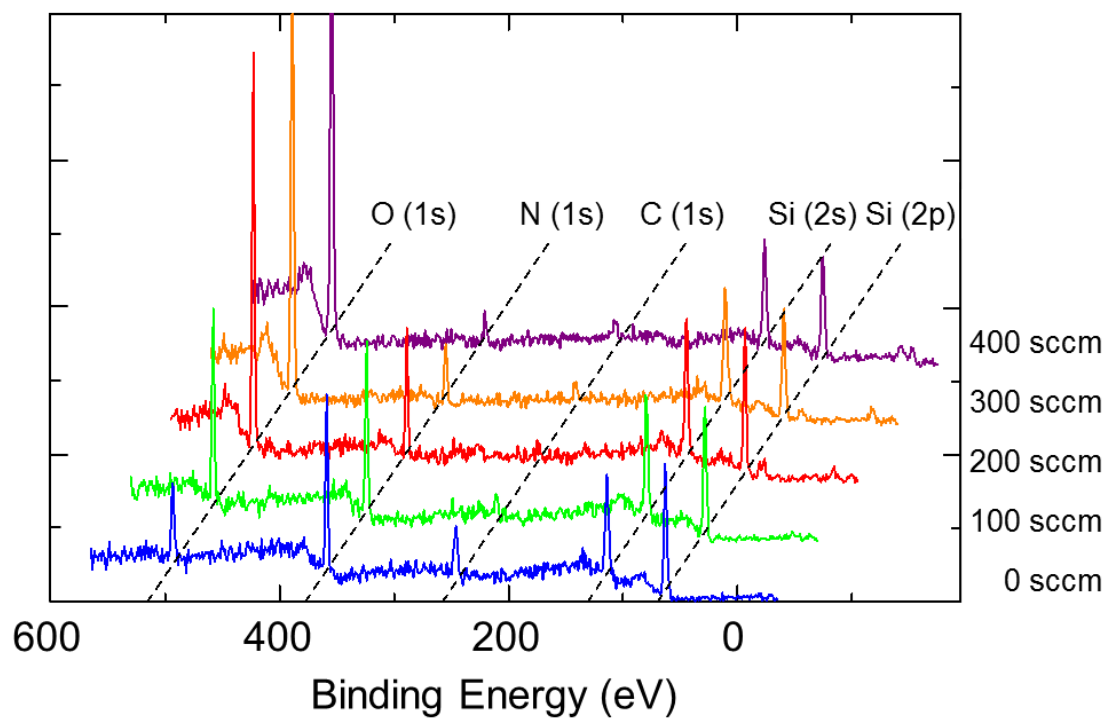


Figure 6 K. Ohdaira *et al.*,